Acta Cryst. (1975). A**31**, 756

Simple Ways of Determining Perovskite Structures

BY A. M. GLAZER

Wolfson Unit for the Study of Phase Transitions in Dielectrics, Cavendish Laboratory, Cambridge, England

(*Received* 2 *May* 1975; *accepted* 9 *May* 1975)

A simple technique is described for ascertaining trial models for the structures of perovskites. The method relies on an understanding of the fundamental components of the structure. Rules are given for determining trial models rapidly.

Introduction

The class of materials known as perovskites is of considerable technological importance, particularly with regard to physical properties such as pyro- and piezo-electricity, dielectric susceptibility, linear and non-linear electrooptic effects. Many of these properties are gross effects, varying enormously from one perovskite to another, and yet the differences in the crystal structures are hardly apparent. The changes in physical properties are particularly large when the external conditions, such as temperature or pressure, are altered. The huge rise in dielectric constant, by as much as a factor of 10^4, found on heating barium titanate is a well known example of this. Generally speaking, such effects occur in connexion with the simultaneous presence of phase transitions in the system, where the atomic structure of the perovskite changes either discontinuously or continuously into another form. In order to be able to understand the origin of the behaviour of the physical properties near phase transitions it is necessary to have as complete a description as possible of what is happening to the atoms in the structure. In the case of the perovskites, because the structural differences between one phase and another are so slight, it can be extremely difficult to carry out a precise structure determination. To the casual worker all perovskites look the same; it is only by a careful study of the splittings of certain X-ray diffraction spots or lines and of the presence of any weak 'extra' (often called difference or superlattice) reflexions, that one can derive a model for the crystal structure. This can be particularly difficult when the splittings of the originally cubic reflexions are small and the difference reflexions arise from weak scatterers. For example, polycrystalline specimens of $PbZr_{0.9}Ti_{0.1}O_3$ show a very small splitting of the powder lines consistent with a rhombohedral distortion of a cube but no difference reflexions (except with neutron diffraction); a single crystal oscillating through 2° for 20 h has been used in our laboratory in order to show their presence. Clearly, such small effects can easily be missed and this accounts for the many incorrect structure determinations of perovskites carried out in the past.

The purpose of this paper is to set out in one place a general method for obtaining a suitable trial model of a particular perovskite, a 'recipe' in effect. The method outlined here will not be suitable for *all* perovskites (which have a habit of doing the unexpected) but it is certainly applicable to a great many of them. The technique has been evolved through many years of experience and owes a great deal to the work of Megaw (1966, 1969, 1971, 1973), who first showed how the structures could be broken up into their various components. These components are:

(i) tilting of the anion octahedra

(ii) displacements of the cations; these can be parallel (ferroelectric structure) or antiparallel (antiferroelectric structure).

(iii) distortions of the octahedra.

These components are also the important parameters involved in the soft modes often found near the phase transitions. Component (iii) is usually associated with component (ii) and so will not be discussed separately here; in any case, distortions are normally of a second-

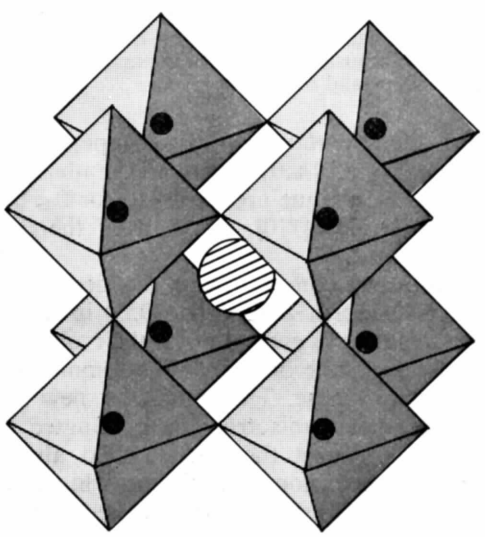

Fig. 1. The ideal cubic (aristotype) perovskite of formula ABX_3 (A, B = cation, X = anion). The anions are at the vertices of the octahedra. Black circles B cations, hatched circle A cation (taken from Megaw, 1973).

order nature. As has been shown earlier (Glazer, 1972), component (i), when it is present, is the most important in establishing the overall space-group symmetry of the particular perovskite.

If the actual kind of tilting can be established then one is well on the way to understanding the diffraction pattern, and it is on this aspect that we shall concentrate. Throughout, unless specifically stated otherwise, all unit cells will be referred to the pseudocubic axes.

Tilting of anion octahedra

In Fig. 1 is shown a diagram of the ideal perovskite (usually the highest-temperature phase), the *aristotype* in Megaw's terminology. When the cations are displaced or the octahedra are tilted (or rotated), different types of structures are produced, *hettotypes*, which are always of lower symmetry than the aristotype. One may ask what happens when a particular octahedron is tilted about some direction; it turns out that there is no unique answer to this. In fact, there are 23 possible simple tilt systems (Glazer, 1972). In this earlier work is was possible to derive a convenient nomenclature for the tilt systems based on breaking the tilting into component tilts about the three pseudocubic axes.

The tilting of the octahedra has several effects which we shall deal with separately.

(*a*) *Unit-cell lengths*

The most important consequence of the tilting is to double certain cell axes. This can be seen in Fig. 2 where the tilt axis is vertically out of the plane of the diagram. The tilting causes the B cation–anion bond in one octahedron to rotate in an opposite direction to that in a neighbouring octahedron, thus giving rise to a doubling of the repeat distances perpendicular to the tilt axis. At the same time if we attempt to maintain the B cation–anion bond distance we must expect the B cation–B cation distance to become shorter and hence reduce the axial lengths. If we denote the angles of tilt about the pseudocubic [100], [010] and [001] directions by α, β and γ respectively (not to be confused with the unit-cell angles), then the new axial lengths are given by

$$a_p = a_o \cos\beta \cos\gamma \quad (1a)$$
$$b_p = a_o \cos\alpha \cos\gamma \quad (1b)$$
$$c_p = a_o \cos\alpha \cos\beta \quad (1c)$$

where a_p, b_p and c_p are the pseudocubic subcell lengths and a_o the cell edge length of the aristotype. The actual repeat distances, of course, are twice these subcell lengths. If we rearrange these equations thus:

$$\frac{a_p}{b_p} = \frac{\cos\beta}{\cos\alpha} \qquad \frac{b_p}{c_p} = \frac{\cos\gamma}{\cos\beta} \qquad \frac{c_p}{a_p} = \frac{\cos\alpha}{\cos\gamma}, \quad (2)$$

it can be seen immediately that equality of any two tilt angles means equality of the cell axes *coincident* with the tilt axes. For example, if the tilts about [100] and [010], *i.e.* α and β, are equal in magnitude then a_p must of necessity be equal to b_p. We have, of course, ignored the effect of distortions of the octahedra in this process, but since it is the tilts that govern the symmetry so much, we can expect that our argument will be reasonable as far as equality or non-equality of tilts/lattice parameters is concerned. It does mean that we cannot expect to use formulae such as (2) to calculate absolute values of the lattice parameters unless we are sure that the distortions are negligible. We therefore see that if the lattice parameters are known we may infer the tilt angles or, at least, whether any two are equal. This only holds true, of course, when there are tilts present; when they are not, the lattice parameters are correlated directly with octahedral distortions normally produced by cation displacements.

In the tilt-system nomenclature, equality of tilt magnitudes is denoted by repetition of the letters appropriate to the particular tilt axes. Thus **aac** means equal tilts about [100] and [010], **aaa** means equal tilts about all three axes, and **abc** means three unequal tilts. These symbols therefore tell us immediately which unit cell axes are equal. In these examples, we have

$$a_p = b_p \neq c_p \text{ for } \mathbf{aac}$$
$$a_p = b_p = c_p \text{ for } \mathbf{aaa}$$

and

$$a_p \neq b_p \neq c_p \text{ for } \mathbf{abc}.$$

(*b*) *Unit-cell angles*

As was shown in the earlier work, there are basically two types of tilt: tilts where the octahedra *along* a tilt axis are tilted *in-phase* about the axis, denoted with the superscript +, and tilts where the octahedra are tilted in *antiphase*, denoted by the superscript −. When there are no tilts about a particular axis, 0 is used. The signs of the tilts are important for determining the lattice type and the unit-cell angles. The latter are correlated with the signs in the following way. Any two + tilts, or one + and one − tilt, mean that the relevant axes are normal to each other; any two − tilts mean that the relevant cell axes are inclined to each other. Thus $\mathbf{a}^-\mathbf{b}^+\mathbf{c}^+$ has three axes of unequal length normal to one another. On the other hand $\mathbf{a}^-\mathbf{a}^-\mathbf{c}^+$ has two equal axes, $a_p = b_p$, which are inclined to each other but which are both normal to c_p. Similarly $\mathbf{a}^-\mathbf{a}^-\mathbf{a}^-$ has three equal axes inclined to one another (obviously with equal angles). In the 1972 paper the space groups of all the 23 possible tilt systems were worked out and for convenience they are repeated here (Table 1).

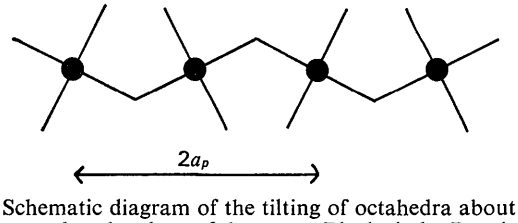

Fig. 2. Schematic diagram of the tilting of octahedra about an axis normal to the plane of the paper. Black circles B cations.

(*c*) *Difference reflexions*

Since tilting of the octahedra causes a doubling of the unit-cell axes, extra reflexions are produced which lie on half-integral reciprocal-lattice planes. With reference now to the 'doubled' unit cell these reflexions can be indexed with some indices odd, whilst the ordinary reflexions (the main reflexions) have all *hkl* even. It turns out, fortunately, that the two types of tilts, in-phase (+) and antiphase (−), result in two distinct classes of difference reflexion. It is a simple matter to show that + tilts give rise to reflexions of the type odd-odd-even, whilst − tilts produce odd-odd-odd reflexions. More specifically we can write the following rules:

$\mathbf{a}^+$ produce reflexions even-odd-odd with $k \neq l$ *e.g.* 013, 031 (3*a*)

$\mathbf{b}^+$ produce reflexions odd-even-odd with $h \neq l$ *e.g.* 103, 301 (3*b*)

$\mathbf{c}^+$ produce reflexions odd-odd-even with $h \neq k$ *e.g.* 130, 310 (3*c*)

$\mathbf{a}^-$ produce reflexions odd-odd-odd with $k \neq l$ *e.g.* 131, 113 (3*d*)

$\mathbf{b}^-$ produce reflexions odd-odd-odd with $h \neq l$ *e.g.* 113, 311 (3*e*)

$\mathbf{c}^-$ produce reflexions odd-odd-odd with $h \neq k$ *e.g.* 131, 311 . (3*f*)

Actually it is possible to go still further and derive the relationships between the intensities of the difference reflexions and the tilt angles, α, β, and γ. These are

$$I(\mathbf{a}^+) \propto (ki^l - li^k)^2\alpha^2 \quad (4a)$$

$$I(\mathbf{b}^+) \propto (-li^h + hi^l)^2\beta^2 \quad (4b)$$

$$I(\mathbf{c}^+) \propto (hi^k - ki^h)^2\gamma^2 \quad (4c)$$

$$I(\mathbf{a}^-, \mathbf{b}^-, \mathbf{c}^-) \propto [(ki^l - li^k)\alpha \pm (-li^h + hi^l)\beta \pm (hi^k - ki^h)\gamma]^2 \quad (4d)$$

where $i = \sqrt{-1}$ and the $\pm$ signs depend on the particular choice of origin for the tilt system (there are two such choices in general, but for the present purposes we shall not need to consider them). The reader will immediately see that these relationships are consistent with the rules given before. Another point worth noting is that + tilts produce Bragg reflexions at reciprocal-lattice points corresponding to the one-face-centred positions, whilst for − tilts they occur at the all-face-centred points. When these tilts arise, as they often do, through the 'freezing-in' of a soft mode at a

Table 1. *Complete list of possible simple tilt systems*

Serial number	Symbol	Lattice centring	Multiple cell	Relative pseudocubic subcell parameters	Space group
Three-tilt systems					
(1)	$\mathbf{a}^+\mathbf{b}^+\mathbf{c}^+$	*I*	$2a_p \times 2b_p \times 2c_p$	$a_p \neq b_p \neq c_p$	*Immm* (No. 71)
(2)	$\mathbf{a}^+\mathbf{b}^+\mathbf{b}^+$	*I*		$a_p \neq b_p = c_p$	*Immm* (No. 71)
(3)	$\mathbf{a}^+\mathbf{a}^+\mathbf{a}^+$	*I*		$a_p = b_p = c_p$	*Im*3 (No. 204)
(4)	$\mathbf{a}^+\mathbf{b}^+\mathbf{c}^-$	*P*		$a_p \neq b_p \neq c_p$	*Pmmn* (No. 59)
(5)	$\mathbf{a}^+\mathbf{a}^+\mathbf{c}^-$	*P*		$a_p = b_p \neq c_p$	*Pmmn* (No. 59)
(6)	$\mathbf{a}^+\mathbf{b}^+\mathbf{b}^-$	*P*		$a_p \neq b_p = c_p$	*Pmmn* (No. 59)
(7)	$\mathbf{a}^+\mathbf{a}^+\mathbf{a}^-$	*P*		$a_p = b_p = c_p$	*Pmmn* (No. 59)
(8)	$\mathbf{a}^+\mathbf{b}^-\mathbf{c}^-$	*A*		$a_p \neq b_p \neq c_p$ $\alpha \neq 90°$	$A2_1/m11$ (No. 11)
(9)	$\mathbf{a}^+\mathbf{a}^-\mathbf{c}^-$	*A*		$a_p = b_p \neq c_p$ $\alpha \neq 90°$	$A2_1/m11$ (No. 11)
(10)	$\mathbf{a}^+\mathbf{b}^-\mathbf{b}^-$	*A*		$a_p \neq b_p = c_p$ $\alpha \neq 90°$	*Pmnb* (No. 62)*†
(11)	$\mathbf{a}^+\mathbf{a}^-\mathbf{a}^-$	*A*		$a_p = b_p = c_p$ $\alpha \neq 90°$	*Pmnb* (No. 62)*†
(12)	$\mathbf{a}^-\mathbf{b}^-\mathbf{c}^-$	*F*		$a_p \neq b_p \neq c_p$ $\alpha \neq \beta \neq \gamma \neq 90°$	$F\bar{1}$ (No. 2)
(13)	$\mathbf{a}^-\mathbf{b}^-\mathbf{b}^-$	*F*		$a_p \neq b_p = c_p$ $\alpha \neq \beta \neq \gamma \neq 90°$	*I*2/*a* (No. 15)*
(14)	$\mathbf{a}^-\mathbf{a}^-\mathbf{a}^-$	*F*		$a_p = b_p = c_p$ $\alpha = \beta = \gamma \neq 90°$	$R\bar{3}c$ (No. 167)
Two-tilt systems					
(15)	$\mathbf{a}^0\mathbf{b}^+\mathbf{c}^+$	*I*	$2a_p \times 2b_p \times 2c_p$	$a_p < b_p \neq c_p$	*Immm* (No. 71)
(16)	$\mathbf{a}^0\mathbf{b}^+\mathbf{b}^+$	*I*		$a_p < b_p = c_p$	*I*4/*mmm* (No. 139)†
(17)	$\mathbf{a}^0\mathbf{b}^+\mathbf{c}^-$	*B*		$a_p < b_p \neq c_p$	*Bmmb* (No. 63)
(18)	$\mathbf{a}^0\mathbf{b}^+\mathbf{b}^-$	*B*		$a_p < b_p = c_p$	*Bmmb* (No. 63)
(19)	$\mathbf{a}^0\mathbf{b}^-\mathbf{c}^-$	*F*		$a_p < b_p \neq c_p$ $\alpha \neq 90°$	*F*2/*m*11 (No. 12)
(20)	$\mathbf{a}^0\mathbf{b}^-\mathbf{b}^-$	*F*		$a_p < b_p = c_p$ $\alpha \neq 90°$	*Imcm* (No. 74)*
One-tilt systems					
(21)	$\mathbf{a}^0\mathbf{a}^0\mathbf{c}^+$	*C*	$2a_p \times 2b_p \times c_p$	$a_p = b_p < c_p$	*C*4/*mmb* (No. 127)
(22)	$\mathbf{a}^0\mathbf{a}^0\mathbf{c}^-$	*F*	$2a_p \times 2b_p \times 2c_p$	$a_p = b_p < c_p$	*F*4/*mmc* (No. 140)
Zero-tilt system					
(23)	$\mathbf{a}^0\mathbf{a}^0\mathbf{a}^0$	*P*	$a_p \times b_p \times c_p$	$a_p = b_p = c_p$	*Pm*3*m* (No. 221)

* These space-group symbols refer to axes chosen according to the matrix transformation

$$\begin{pmatrix} 1 & 0 & 0 \\ 0 & \frac{1}{2} & -\frac{1}{2} \\ 0 & \frac{1}{2} & \frac{1}{2} \end{pmatrix}.$$

† In the 1972 paper tilt systems (10) and (11) were incorrectly given the space-group symbol *Pnma* and tilt system (16) the symbol *I*4/*m*.

phase transition, the relevant mode is one with wave vector $\mathbf{q}=(\frac{1}{2}\frac{1}{2}0)$ for + tilts and $\mathbf{q}=(\frac{1}{2}\frac{1}{2}\frac{1}{2})$ for − tilts. This is often described as the condensation of a phonon at the M and R points respectively of the Brillouin zone.* We see then that this system of tilt components is naturally related to the normal modes of vibration which are so important near a phase transition.

Cation displacements

It is considerably more difficult to give any hard-and-fast rules for the cation displacements. Sometimes half-integral difference reflexions (or odd indices on the doubled pseudocubic cell) occur which do not conform to the tilt reflexions, in which case it is relatively easy to infer the type of displacement. Clearly this can only occur when they are antiparallel; when they are parallel, however, no difference reflexions are produced. The most reliable indication of the displacements is often given by the space group due to the tilt system, particularly if it is known whether the particular substance is centrosymmetric or not. If the displacements are antiparallel the structure is centrosymmetric and we normally find that the space group is the same as that for the tilt system alone. When they are parallel, the structure is non-centrosymmetric and the space group is a subgroup of that for the tilt system. It is therefore relatively easy to suggest the most likely space group for the structure and since the A and B cations usually lie at special positions we often know the displacement directions.

When there are no tilts present, as evidenced perhaps by the lack of the necessary difference reflexions, the displacements can often be ascertained from the unit-cell geometry. Thus if the unit cell is a rhombohedral distortion of the aristotype cell, and no difference reflexions are found, it is reasonable to suppose that the structure has parallel cation displacements along [111] (the threefold axis) with space group $R3m$. The lowest-temperature phase of $BaTiO_3$ is an example of this (Rhodes, 1949; Kay & Vousden, 1949).

One must be careful here, however. It is possible to have distortions of the octahedra even when there are no displacements or tilts. $KCuF_3$ is an example of this (Okazaki & Suemune, 1961), where Jahn–Teller effects distort the octahedra to produce a tetragonal structure. Fortunately this type of structure is very rare and in any case might well be expected since it is well known that $Cu(d^9)$ shows strong Jahn–Teller distortion.

Examples

Let us consider some examples of known perovskite structures in order to see how the technique described can be applied in practice.

* With the origin chosen at the centre of the octahedra the irreducible representations for these modes are conventionally labelled M_3 and R_{25}.

(*a*) *The high-temperature phases of* $NaNbO_3$

Above room temperature, $NaNbO_3$ possesses six phases. For the present purposes we shall consider the four highest phases, labelled S, T_1, T_2 and cubic. Lattice-parameter measurements (Glazer & Megaw, 1973) gave the following results:

480–520 °C S	$a_p\neq b_p\neq c_p$	all axes orthogonal.
520–575 °C T_1	$a_p\neq b_p\neq c_p$	
575–641 °C T_2	$a_p=b_p<c_p$	
> 641 °C Cubic	$a_p=b_p=c_p$	

Weissenberg photographs of the first half-integral reciprocal-lattice layers of phase T_2 (Glazer & Megaw, 1972), showed the presence of only three, very weak difference reflexions, $\frac{1}{2}\frac{3}{2}0$, $\frac{1}{2}\frac{3}{2}1$ and $\frac{1}{2}\frac{5}{2}0$ (130, 131 and 150 on a pseudocubic cell $2a_p\times 2b_p\times c_p$). Since these reflexions occur at low angles it is likely that they arise from the O atoms and as they are of the odd-odd-even type the tilt system (No. 21) $\mathbf{a}^0\mathbf{a}^0\mathbf{c}^+$ is immediately suggested.† The space group from Table 1 is $C4/mmb$ and, being tetragonal, is consistent with the measured unit-cell geometry. Trivially, two equal (zero-magnitude) tilts mean two equal axes. The initial determination of the trial structure in this case took approximately five minutes allowing for indexing. Subsequent calculations of structure factors confirmed this structure.

Similar photographs of phase T_1 (Ahtee, Glazer & Megaw, 1969) showed the following reflexions 310, 130, 131, 151, 312, and 113 (on the doubled cell $2a_p\times 2b_p\times 2c_p$). It was possible to infer from this that these were tilt reflexions which could be broken down into the following:

310, 130, 312	$\mathbf{c}^+$ tilt	(odd-odd-even)
131, 151	$\mathbf{a}^-$ tilt	(odd-odd-odd).

Reference to (3) shows that there is neither a $\mathbf{b}^+$ nor a $\mathbf{b}^-$ tilt. This suggests structure (No 17) $\mathbf{a}^-\mathbf{b}^0\mathbf{c}^+$ with space group $Ccmm$; this orthorhombic space group is again consistent with the lattice parameter measurements. We have three unequal tilts and three unequal lattice parameters.

Finally in phase S, the reflexion 510 was observed (Glazer & Ishida, 1974) in addition to the above reflexions, suggesting a $\mathbf{b}^+$ tilt. This gives the structure of phase S as (No. 4) $\mathbf{a}^-\mathbf{b}^+\mathbf{c}^+$ with space group $Pnmm$, with unit-cell geometry again consistent with the measured lattice parameters. The four phases are summarized thus

$$\mathbf{a}^-\mathbf{b}^+\mathbf{c}^+(S)\overset{520^\circ C}{\rightleftharpoons}\mathbf{a}^-\mathbf{b}^0\mathbf{c}^+(T_1)\overset{575^\circ C}{\rightleftharpoons}$$
$$\mathbf{a}^0\mathbf{a}^0\mathbf{c}^+(T_2)\overset{641^\circ C}{\rightleftharpoons}\mathbf{a}^0\mathbf{a}^0\mathbf{a}^0\ \text{(cubic)},$$

showing the progressive loss of tilts one by one as the temperature is raised.

† Note that in this tilt system one of the unit-cell axes is not doubled.

(*b*) *The room-temperature structure of* $CaTiO_3$

The structure of $CaTiO_3$ was determined by Kay & Bailey (1957) from single-crystal data. Here we shall consider the powder diagram and see how much can be inferred from it. From the splittings of the main reflexions it can easily be determined that

$$a_p = b_p \neq c_p \quad \gamma \neq 90° .$$

The fact that the angle between the a_p and b_p axes is different from 90° suggests two antiphase tilts (from the rules given earlier) and the equality of a_p and b_p further suggests that the tilt angles are equal. Two possibilities arise, (No. 10) $\mathbf{a^-a^-c^+}$ or (No. 20) $\mathbf{a^-a^-c^0}$ (space groups *Pbnm* and *Imam* respectively), as given in Table 1. Examination of the difference reflexions in the powder diffraction pattern allows one to classify the reflexions into classes, and Table 2 can be constructed. We see that the presence of 00*l*-type reflexions supports the $\mathbf{a^-a^-c^+}$ system.

In Table 2 no attempt has been made to consider the signs of the *hkl*, except where absolutely necessary. Note that in the last column, tilt system $\mathbf{a^-a^-c^+}$ has been used to index certain difference reflexions, the remaining ones, $N = 13$, 17 and 29 not being consistent with any tilt type. It is natural, therefore, to suggest that these reflexions arise from antiparallel cation displacements.

We can get some idea of the directions of the cation displacements in the following way. Consider Fig. 3 which shows schematically the tilt arrangement $\mathbf{a^-a^-c^+}$. The displacement of the Ca atom will be linked to a great extent to its environment by simple steric principles. Let us examine the environment of the Ca atom marked A. Firstly, of the O atoms numbered 5, 6, 7 and 8 the closest are 5 and 8 since they are displaced towards the Ca atom, thus tending to push it along [010]. Secondly, of the O atoms 9, 10, 11 and 12 number 12 is closest to the Ca atom and thus tends to push it along $[\bar{1}\bar{1}0]$. O atoms 1, 2, 3 and 4, however, are not sufficiently close to the Ca atom to affect its position much. We see, then, that two O atoms push the Ca along [010] and one along $[\bar{1}\bar{1}0]$. To a gross approximation we find that the resultant vector displacement is

$$2[010] + [\bar{1}\bar{1}0] = [\bar{1}10] .$$

Proceeding in a similar manner with the remaining Ca atoms, we arrive at the arrangement of displacements shown in Fig. 3. If we now assume that the tilt-system space group is the same as that of the crystal (*Pbnm*), with the origin half-way between Ca atoms along [001], it is easily seen that the Ti atoms are not displaced at all, as they lie on centres of symmetry. It is worth noting that there is an alternative choice of origin for this structure. We could place the Ca atoms on centres of symmetry and then the Ti atoms would have freedom to be displaced. This is a less likely structure since it ignores the steric effects of the O atoms on the Ca atom. We conclude, therefore, that the cation displacements must lie approximately along the $\langle 1\bar{1}0 \rangle$ pseudocubic directions (the $\langle 010 \rangle$ directions of the orthorhombic cell) in antiparallel sheets perpendicular to [001]. The extra reflexions, therefore must have *l* odd and hence they are

N	*hkl*
13	023, 203
17	401, 041
29	025, 205 .

Reference to Kay & Bailey (1957) shows that our structure is correct and, in fact, their refinement resulted in Ca atoms displaced *exactly* along the $\langle 1\bar{1}0 \rangle$ pseudocubic directions (in some other perovskites with the same type of structure the A cations are not displaced exactly along these directions, although they are always fairly close to them).

(*c*) *The structure of* $PbZr_{0.9}Ti_{0.1}O_3$

In Fig. 4 is shown the neutron diffraction pattern from a polycrystalline sample of $PbZr_{0.9}Ti_{0.1}O_3$. Apart from a few extra reflexions the pattern looks very much like that from a primitive cubic structure. However the higher resolution found in X-ray photographs shows that reflexions such as *hhh* are split whilst *h*00 are not. From this we infer that the symmetry is probably rhombohedral. It is known that the material is a ferroelectric and so the cations are displaced in a parallel fashion, obviously along the threefold axis. The extra reflexions shown in the neutron profile do not appear in the X-ray photographs since they arise from the O

Table 2. *Indexing of the powder pattern for* $CaTiO_3$

$N = h^2+k^2+l^2$ (Pseudocubic subcell)	$N = h^2+k^2+l^2$ (Doubled cell)	Type	Tilt	*hkl* for $\mathbf{a^-a^-c^+}$
$2\frac{1}{2}$	10	*ooe*, *oeo* or *eoo*	+	310, 130
$2\frac{3}{4}$	11	*ooo*	−	311, 131, 113
$3\frac{1}{4}$	13	*oee*, *eoe* or *eeo*		
$3\frac{1}{2}$	14	*ooe*, *oeo* or *eoo*	+	312, 132
$4\frac{1}{4}$	17	*oee*, *eoe* or *eeo*		
$4\frac{3}{4}$	19	*ooe*, *oeo* or *eoo*	+	$\bar{3}30$
$5\frac{1}{2}$	22	*ooe*, *oeo* or *eoo*	+	$\bar{3}32$
$7\frac{1}{4}$	29	*oee*, *eoe* or *eeo*		
$8\frac{3}{4}$	35	*ooo*	−	531, 513, 135 ...

o = odd *e* = even.

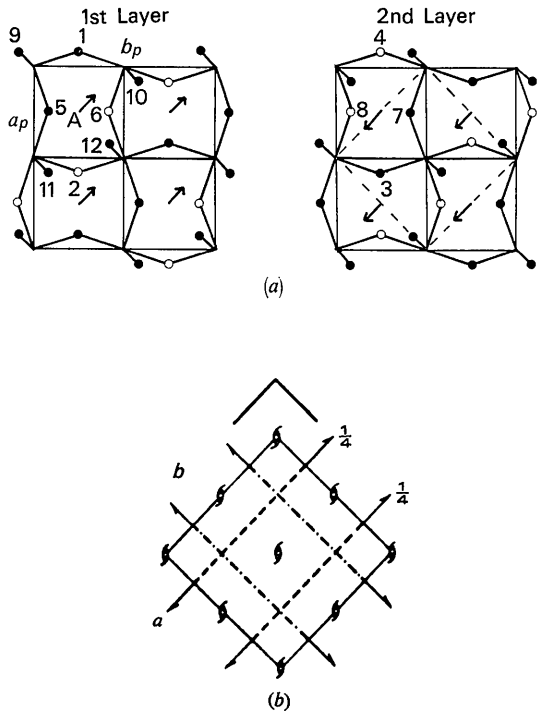

Fig. 3. (*a*) The structure of $CaTiO_3$. Full circles denote O atoms above the plane of the diagram whilst open circles are those below. Arrows indicate the directions of Ca displacements (at height $\frac{1}{4}c$); Ti atoms are at the centres of the octahedra. The dashed cell is the true crystallographic cell with space group *Pbnm*. (*b*) Symmetry elements of space group *Pbnm*.

atoms which do not scatter X-rays strongly enough. It is a very simple matter to index them as 311, 511 *etc.* (on a doubled cell $2a_p \times 2b_p \times 2c_p$) and taking the probable rhombohedral symmetry into account we expect the tilt system to be (No. 14) $\mathbf{a}^-\mathbf{a}^-\mathbf{a}^-$ with symmetry $R\bar{3}c$. The parallel cation (Pb and Zr/Ti) displacements mean that the space-group symmetry will be $R3c$, and this agrees with the earlier derivation by Michel, Moreau, Achenbach, Gerson & James (1969). Fig. 4, incidentally, shows the observed and calculated profiles computed with the profile refinement technique (Rietveld, 1969). On heating the powder, the extra reflexions are lost but the symmetry remains rhombohedral and the material is still ferroelectric. This means that the tilts are lost but the displacements remain to give space group $R3m$. Finally at a higher temperature the symmetry becomes cubic and the displacements disappear to give the paraelectric phase. The whole series can be described by

$$\begin{array}{ccc} \mathbf{a}^-\mathbf{a}^-\mathbf{a}^-(R3c) & & \mathbf{a}^0\mathbf{a}^0\mathbf{a}^0(R3m) \\ [111]\text{ displacements} & \rightarrow & [111]\text{ displacements} \\ & & \rightarrow \mathbf{a}^0\mathbf{a}^0\mathbf{a}^0(Pm3m)\,. \end{array}$$

Conclusion

It can be seen that by breaking the perovskite structure into simple components it is often possible to simplify greatly the task of ascertaining a trial model for the structure of these pseudosymmetric materials. The technique described works well for the vast majority

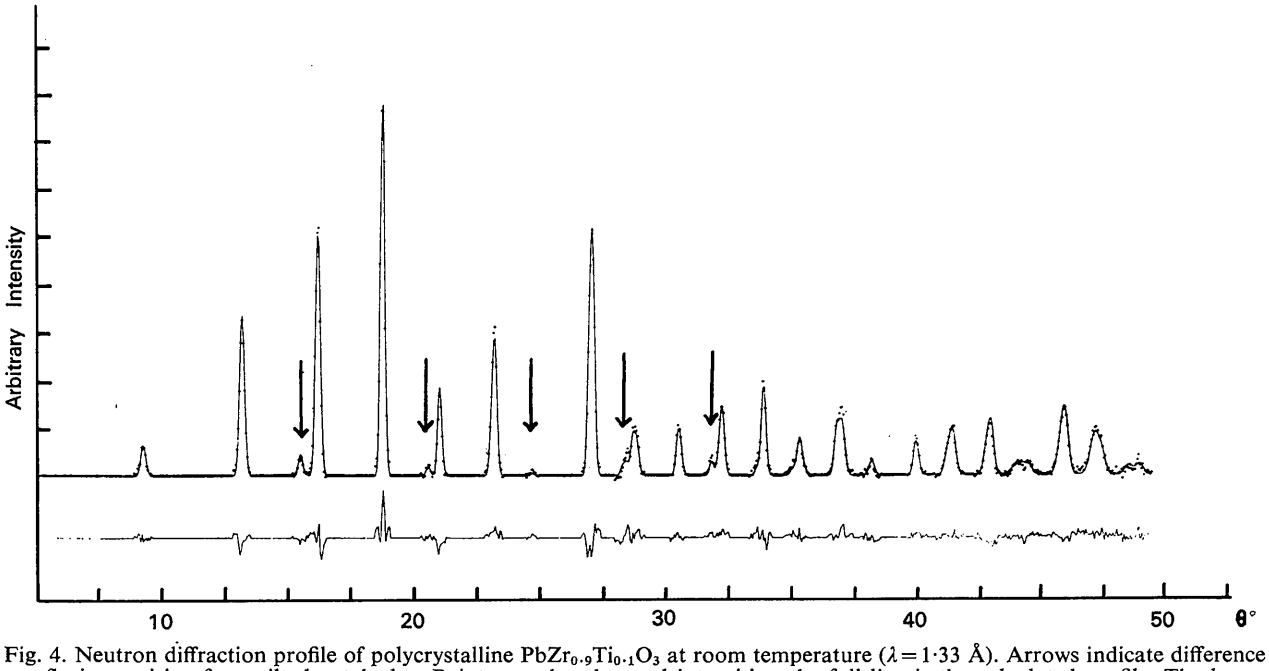

Fig. 4. Neutron diffraction profile of polycrystalline $PbZr_{0.9}Ti_{0.1}O_3$ at room temperature ($\lambda = 1{\cdot}33$ Å). Arrows indicate difference reflexions arising from tilted octahedra. Points are the observed intensities, the full line is the calculated profile. The lower trace shows the difference between observed and calculated intensities (Glazer & Clarke, unpublished).

of perovskites. In fact the only perovskites known to the author in which difficulty would occur are $NaNbO_3$ (phases *P* and *R*), $PbZrO_3$, possibly $AgNbO_3$ and $AgTaO_3$, and $KCuF_3$. In the last case the difficulty, as mentioned earlier, is the large Jahn–Teller distortion of the octahedra which dominates the symmetry. In the other cases, the difficulty lies in the fact that the tilt systems are not simple ones, but consist of combinations of the simple systems. However, even here it is possible to go some way towards deriving the correct structure, but great care is needed when attempting this. Fortunately such structures seem to be quite rare.

At present this general method is being used to analyse the complex sequence of phases in the system $Na/KNbO_3$ with considerable success. A preliminary note of this work has already been published (Ahtee & Glazer, 1974) in which tentative suggestions for the various structures have been made. Since then, many of these have been verified (manuscript in preparation), and this has shown that reliable trial models can be obtained very quickly even when there are many possible phases within a single solid-solution series.

I thank Dr H. D. Megaw for introducing me to the fascinating complexities of the perovskite structure, and the Wolfson Foundation for funds enabling this work to be carried out.

References

AHTEE, M. & GLAZER, A. M. (1974). *Ferroelectrics*, **7**, 93–95.

AHTEE, M., GLAZER, A. M. & MEGAW, H. D. (1969). *Phil. Mag.* **26**, 995–1014.

GLAZER, A. M. (1972). *Acta Cryst.* B**28**, 3384–3392.

GLAZER, A. M. & ISHIDA, K. (1974). *Ferroelectrics*, **6**, 219–224.

GLAZER, A. M. & MEGAW, H. D. (1972). *Phil. Mag.* **25**, 1119–1135.

GLAZER, A. M. & MEGAW, H. D. (1973). *Acta Cryst.* A**29**, 489–495.

KAY, H. F. & BAILEY, P. C. (1957). *Acta Cryst.* **10**, 219–226.

KAY, H. F. & VOUSDEN, P. (1949). *Phil. Mag. Ser.* 7, **40**, 1019–1040.

MEGAW, H. D. (1966). *Proceedings of the International Meeting on Ferroelectricity, Prague*, Vol. 1, pp. 314–321.

MEGAW, H. D. (1969). *Proceedings of the European Meeting on Ferroelectricity, Saarbrücken*, pp. 27–35.

MEGAW, H. D. (1971). *Abstracts of the Second European Meeting on Ferroelectricity, Dijon*: *J. de Phys.* (1972). **33**, C2. 1–C2. 5.

MEGAW, H. D. (1973). *Crystal Structures*: *A Working Approach*. Philadelphia: Saunders.

MICHEL, C., MOREAU, J.-M., ACHENBACH, G., GERSON, R. & JAMES, W. J. (1969). *Solid State Commun.* **7**, 865–868.

OKAZAKI, A. & SUEMUNE, Y. (1961). *J. Phys. Soc. Japan*, **16**, 176–183.

RHODES, R. G. (1949). *Acta Cryst.* **2**, 417–419.

RIETVELD, H. M. (1969). *J. Appl. Cryst.* **2**, 65–71.

Acta Cryst. (1975). A**31**, 762

Calculation of *E* values by Means of the Origin Peak in the Patterson Function

BY KURT NIELSEN

Chemistry Department B, Technical University of Denmark, DK-2800 *Lyngby, Denmark*

(*Received* 17 *March* 1975; *accepted* 19 *March* 1975)

The origin peak in the Patterson function may be used to construct *E* values when the number and type of the atoms in the structure are known. This is illustrated by an example leading to an agreement value between the observed and calculated *E* values of 0·170. For comparison, a least-squares calculation of the best overall anisotropic temperature factor results in an *R* of 0·167. The result obtained from a Wilson plot is 0·188.

Introduction

The origin peak in the Patterson function obeys the point-group symmetry of the Patterson function, and can therefore be expanded in harmonic functions of the appropriate symmetry. If the origin peak, deconvoluted with respect to thermal motion, is known, an analysis of the terms in the expansion will provide some information about the overall anisotropic thermal movements. The applied method of analysis, revealing this information, follows closely the technique used in the analysis of the deformations of atoms (Kurki-Suonio & Meisalo, 1967; Kurki-Suonio, 1967, 1968).

Description of the method

The square of the overall temperature factor is written as

$$T(\mathbf{H}) = \sum_{n,\alpha} T_{n\alpha}(H) K_{n\alpha}(\theta_{\mathbf{H}}, \varphi_{\mathbf{H}}) .$$

The $K_{n\alpha}$ form a complete set of orthonormal harmonic functions adapted to the symmetry of the Patterson function, and H, $\theta_{\mathbf{H}}$ and $\varphi_{\mathbf{H}}$ are the spherical coordinates of the reciprocal-lattice vector **H**. The functions $T_{n\alpha}(H)$ are then calculated from the expression

$$T_{n\alpha}(H) = (4\pi)^2 V^{-1} \sum_{\mathbf{G}} A(\mathbf{G}) K^*_{n\alpha}(\theta_{\mathbf{G}}, \varphi_{\mathbf{G}}) \times \int_0^r j_n(2\pi H u) j_n(2\pi G u) u^2 \mathrm{d}u . \quad (1)$$